Electronic Materials Letters, Vol. 8, No. 4 (2012), pp. 435-443
DOI: 10.1007/s13391-012-2021-2

Charge Carriers and Excitons Transport in an Organic Solar Cell-Theory and Simulation

Ali. Shahini* and Karim. Abbasian

School of Engineering Emerging Technologies, University of Tabriz, Tabriz 51664, Iran

(received date: 24 February 2012 / accepted date: 3 April 2012 / Published date: August 2012)

An organic solar cell model is developed that consists of both excitonic and classical bipolar aspects of solar cells. In order to achieve this goal, the photon recycling term is imported into the equations to connect the Shockley-Queisser theory and the classical diode theory. This model for excitonic and classical bipolar solar cells can describe the combined transport and interaction of electrons, holes and excitons. For high mobilities this model reproduces the Shockley Queisser efficiency limit. We show how varying the respective mobilities of the different species changes the operation mode of the solar cell path between excitonic and bipolar. Then, the effect of conduction band offset on transport will be described in this paper. Finally, validity of reciprocity theorem between quantum efficiency and electroluminescence in this model will be discussed.

Keywords: mobility, exciton, photon recycling, dissociation lifetime

1. INTRODUCTION

In recent years, research has expanded[1,2] from p-n-junction type silicon solar cells to completely different materials and working principles of the photovoltaic device like organic[3-9] or dye sensitized[10-13] solar cells. The evolutionary process of solar cell research leading to state-of-the-art solar cells had economic success while creating a wish for revolutionary progress in research. No longer are only those technologies pursued that seem to work nearly immediately. Instead, theoretical concepts are sought after and materials and devices are designed[14] that may provide the basis for future solar cell generations.

Initial efficiencies of many devices using new concepts are rather low, while the number of scientific disciplines involved and the number of scientific aspects to be considered is fairly high. The introduction of organic materials as photovoltaic absorbers in organic[15] or dye-sensitized solar cells has raised questions whether or not these new types of devices can be described with the help of theories that initially have been developed for inorganic solid-state type devices usually provided with a *p-n*-homo- or heterojuncion. However, so far, these so-called second generation[16] thin-film solar cells have not yet lived up to expectations. They all fall short of achieving the efficiencies reached with conventional first-generation silicon solar cells. Of course, the absorption of light is only the first step to the successful conversion of optical into electrical energy, the photo-generated charge carriers also need to be separated before they recombine. Obviously, this requires high carrier lifetimes. However, one factor which is often overlooked in this context is the importance of charge carrier transport. Within these years, our understanding of this device, its working principles, and its processing has obviously achieved a high degree of maturity. Recently, it has been proposed[17,18] to distinguish between two different concepts of solar cells, namely, the classical inorganic solar cells and the excitonic solar cells usually made from organic absorber materials. However, the overall functionality in all solar cells, namely, the generation of electrical power from solar light, is identical, and there should be a common theory that is valid for all devices on a certain level of abstraction from physical details. The present paper proposes a model that allows us to describe virtually all single-absorber solar cells. For the bulk of the absorber, we use a set of differential equations for excitons, electrons, and holes that is coupled by the dissociation of excitons into an electron/hole pair and the recombination of this pair into an exciton. This approach is similar as in.[19,20] At the surfaces of the absorber, we allow for cross-dissociation of the exciton into an electron in the absorber and a hole in the contact and vice versa.

The paper is organized as follows. We start with a discussion of our model and show how incorporating the photon recycling (PR) term into the equations would result to a self-consistent model that is capable of describing the transport in

*Corresponding author: ali.shahini.62@gmail.com

all existing devices. The theoretical part will be concluded by discussion about reciprocity theorem between quantum efficiency and electroluminescence. The discussion of the results starts with simulation of excitons distributions inside the cell for different exciton dissociation lifetimes, and then we discuss the short-circuit current density of p-i-n-type solar cells for different charge carrier mobilities. Eventually, the dependence of photovoltaic parameters on band offset and the reciprocity validity will be discussed.

2. MODEL

In this section, we will review the way to obtain proposed model for excitionic and bipolar solar cells. Then, we will discuss about the different exciton dissociation processes which exist inside the cell and the related equation as boundary conditions for differential equations to suggest our model for p-i-n-type cells. Finally, in the next subsection, we will provide a discussion about the validity of reciprocity relation between electroluminescence and quantum efficiency.

2.1 P-i-n-type solar cells

Most models currently used for the theoretical description of real solar cells are in flat contradiction to the Shockley-Queisser (SQ)[21] approach. For instance, the most common textbook example for a solar cell[22] uses Shockley's diode theory.[23] The discrepancy between Shockley's diode equation and the SQ theory was addressed by Martí *et al.*.[24] The same authors also pointed out that this contradiction is eliminated by the inclusion of PR, i.e., the process of radiative recombination of an electron and/or hole pair followed by the reabsorption of the photon elsewhere in the absorber. Thus, PR introduces a nonlocal radiative interaction term that complements charge carrier transport and establishes the internal and external radiation balance of the photovoltaic absorber. This effect of optical coupling in the absorber is used to combine SQ theory and the classical diode theory for transport of charge carriers.[25] In order to drive the current densities for electrons, holes and excitons, we have to calculate first the carrier and exciton concentrations. To calculate the carrier and exciton concentrations as a function of depth in the absorber, four differential equations have to be solved, namely, Poisson equation $\Delta\varphi = -\rho/\varepsilon$, relating the electrical potential φ to the space charge ρ and the dielectric constant ε, and three continuity equations for electrons, holes and excitons.

$$D_\chi \frac{d^2\chi}{dx^2} = \frac{\chi}{\tau_D} + \frac{\chi}{\tau_r} - R_\chi np - g_\chi \tag{1}$$

$$D_n \frac{d^2 n}{dx^2} + F\mu_n \frac{dn}{dx} = -\frac{\chi}{\tau_D} + R_\chi np \tag{2}$$

$$D_p \frac{d^2 p}{dx^2} - F\mu_p \frac{dp}{dx} = -\frac{\chi}{\tau_D} + R_\chi np \tag{3}$$

Here, g_χ is the optical generation rate for excitons, R_χ is the recombination rate of free carriers leading to the creation of excitons, τ_D is the bulk dissociation lifetime of the excitons, τ_r is the radiative lifetime of the excitons, F is the electric field, $\mu_{\chi/n/p}$ are the mobilities, and $D_{\chi/n/p} = \mu_{\chi/n/p}\, kT/q$ are the diffusion constants according to Einstein's equation, where kT is the thermal energy and q is the elementary charge. There are two exciton dissociation processes inside the cell, the bulk dissociation mechanism and the interface dissociation mechanism which are defined by the bulk dissociation lifetime τ_D. Note at this point that, due to the finite cell thickness, a recombination event in the volume of the photovoltaic absorber does not necessarily lead to an emission of a photon from the surface of the solar cell. Instead the possibility of re-absorption of this photon by generation of another exciton has to be considered even in equilibrium[25] which is used in this paper to involve the PR effect into our calculations. After generation, the excitons can dissociate into electrons and holes in the bulk of the absorber. This dissociation as well as the recombination of electrons and holes and creation of excitons are interlinked by $R_x n_0 p_0 = x_o/\tau_D$ where n_0, p_0 and x_0 denote the equilibrium concentrations of electrons, holes and excitons respectively. In the nonequilibrium situation, the interface dissociation and recombination process defines the boundary condition for the continuity equations, $H_n n_{j0} p_{b0} = S_{xn} x_0$, where the equilibrium concentrations of electrons and holes in the junction and bulk are denoted by n_{j0} and p_{b0}. The exciton current density at the cordinate $x = 0$ is defined by $j_\chi = S_{\chi n} n(0) - H_n n_j p(0)$. Similarly, j_n is defined by $j_n = S_n n(0) - S_n^* n_j$ such that j_n corresponds to the net number of free electrons collected by the junction at $x = 0$ whereas j_χ counts the number of excitons that are separated into electrons (in the junction) and holes (in the bulk) at that interface (Fig. 1). Because of our assumption that excitons only disso-

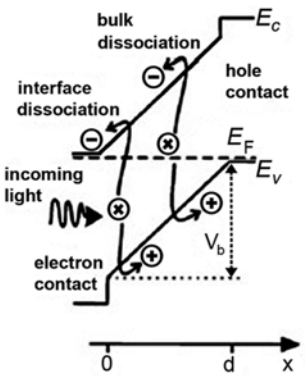

Fig. 1. Scheme of the p-i-n-junction device. The photogenerated exciton can be either split in the bulk (bipolar case) or at the junction (excitonic case) of the device.

ciate at the light exposed surface of the absorber ($x = 0$), the hole current density (analyzed at $x = d$) corresponds to the sum $j_p = j_n + j_\chi$. The collection of free electrons at the interface is determined by $S_n^* n_j = S_n n_b$. Here H_n is cross recombination rate of electrons in the junction with holes in the bulk of the absorber, $S_{\chi n}$ is dissociation velocity of excitons at the electron contact, and S_n, S_n^* have the dimension of a (collection or injection) velocity. Note that in a p-i-n-type structure the electrical field F results from the difference between the built-in potential V_b (cf. Fig. 1) and the applied external voltage V according to $F = (V_b - V)/d$ where d is the thickness of the intrinsic (undoped) absorber layer as sketched in Fig. 1.

2.2 Reciprocity between photovoltaic quantum efficiency and electroluminescence

The assumptions defining a cell in the SQ-limit are perfect absorption with each photon creating exactly one electron/hole pair, perfect collection of carriers and radiative recombination as the only allowed recombination mechanism which result to high mobility and thus flat quasi-Fermi level. In this situation the emitted photon flux ϕ_{em} under the applied voltage bias V is

$$\phi_{em}(V,E) = \frac{2\pi E^2}{h^3 c^2} \frac{A(E)}{[\exp((E - qV)/kT) - 1]} \tag{4}$$

Where h is the Planck constant, c the velocity of light in vacuum, $A(E)$ is the absorptance and emissivity of the solar cell, and kT is the thermal energy. For voltages that are small compared with the emitted photon energies, i.e. $E - qV >> kT$, we can simplify Eq. (4) to

$$\phi(V,E) = A(E)\phi_{bb}\exp(qV/kT) \tag{5}$$

Where the black body spectrum ϕ_{bb} is defined by

$$\phi_{bb} = \frac{2\pi E^2}{h^3 c^2}\exp\left(\frac{-E}{kT}\right) \tag{6}$$

In the SQ limit the radiative saturation current density derived from Eq. (4) is

$$J_{0,rad} = q\int_0^\infty A(E)\phi_{bb}(E)dE \tag{7}$$

And maximum short circuit current density would be

$$J_{Sc,rad} = q\int_0^\infty A(E)\phi_{sun}(E)dE \tag{8}$$

Where ϕ_{sun} denotes the spectral photon flux arriving from the sun at the cell's surface.

For arbitrary values of the mobility and thus nonconstant quasi-Fermi levels, the injection and radiative recombination as well as photogeneration and collection must be included into the connection between light absorbing and light emitting. The Donoalto theorem[26,27] provides this relation that connects the injection of carriers in the dark to the extraction of carriers under illumination. Combining the two pairs, absorption-collection (for the photovoltaic situation) and injection-emission (for the LED situation), a reciprocity relation between external photovoltaic quantum efficiency Q_e and electroluminescent emission ϕ_{em} has been derived, stating that

$$\phi_{em}(E) = Q_e(E)\phi_{bb}(E)\left[\exp\left(\frac{qV}{kT}\right) - 1\right] \tag{9}$$

This equation implies that the information contained in the EL spectrum equals that in the quantum efficiency. However, the multiplication with the black body spectrum, which decays exponentially for higher energies, weighs the quantum efficiency in such a way that the quantum efficiency can be derived experimentally from the EL emission only in the energetic region around the band gap.

Now the emitted and absorbed portion of the light is given by the external quantum efficiency and no longer by the absorptance. Thus it follows for the radiative limit of the saturation current density,

$$J_{0,rad} = q\int_0^\infty Q_e(E)\phi_{bb}(E)dE \tag{10}$$

As well as the short circuit current density,

$$J_{Sc,rad} = q\int_0^\infty Q_e(E)\phi_{sun}(E)dE \tag{11}$$

And of the open circuit voltage,

$$V_{oc,rad} = \frac{kT}{q}\ln\left(\frac{J_{Sc,rad}}{J_{0,rad}} + 1\right) \tag{12}$$

Which show that the validity of the reciprocity relation, Eq. (9), directly correlates with the voltage dependence of carriers and excitons collection and injection. This is because the different spectral dependence of $\phi_{bb}(E)$ and $\phi_{sun}(E)$ in Eqs. (10) and (11) will weigh the different spectral parts of $Q_e(E)$ differently. However, the resulting changes will be small because the ratio $J_{Sc,rad}/J_{o,rad}$ enters only logarithmically into V_{oc}. In the next section, we will discuss cases where voltage-dependent collection causes the fill factor FF = $\max(-JV)/(J_{SC,rad}V_{oc,rad})$ to decrease although the open circuit voltage remains virtually unaffected. Voltage-dependent carrier collection violates also the assumptions required for the derivation of the reciprocity relation [Eq. (9)]. With this model, we can compare EL emission and the external quantum efficiency, which allows us to test whether or not a given configuration is compatible with the electro-optical reciprocity. We explicitly investigate the validity of reciprocity in the next Section and check whether a connection between this validity and the fill factor losses due to voltage-dependent collection exists.

Table 1. Constant parameters for a p-i-n type solar cell. V_{bi} is equilibrium built-in potential inside the absorber and χ_0 is the equilibrium concentration of excitons.

Constant parameters				
Thickness (d)	Intrinsic carrier concentration (n_i)	Equilibrium bilt-in potential (V_{bi})	Recombination lifetime (τ_r)	Equilibrium exciton concentration (χ_0)
300 nm	10^3 cm^{-3}	1.3 V	200 μs	4.4×10^{-3} cm^{-3}

3. RESULTS AND DISCUSSION

In this section the results of simulation are provided. In this way, we use matlab to solve the differential equations with the mentioned self-consistent method.

In order to focus on the charge transport mechanism in excitonic and bipolar solar cells, the following computations are restricted to the short circuit situation of p-i-n-type solar cells. Also, for all simulations we have used a set of constant parameters, which are shown in Table 1. The absorption coefficient of ZnPc as a typical organic absorber material (taken from Fig. 4 in[28]), an optical generation profile, and a photon recycling scheme calculated according to[25] that both result from a Lambertian cell surface. As we will see this absorption coefficient will result to a maximum short circuit current density $J_{Sc,max} = 20.5$ mAcm^{-2} under illumination with an AM1.5G solar spectrum. Also, the radiative recombination of excitons is the only loss mechanism considered throughout this paper.

In first step, we show that this model is able to describe a continuous transition from a situation where transport is basically arranged by excitons and a situation where transport is exclusively supported by electrons and holes. We achieve this transition by a variation of the dissociation lifetime, τ_D, from 10^{-4} s to 10^{-9} s. We can see how this range of τ_D affects the excitonic contribution $J_x = -qj_x(0^+)$ and the bipolar contributions $J_n = -qj_n(0^+)$ and $J_p = qj_p(d)$ to the photocurrent. Figure 2 depicts distribution of excitons inside the cell for low exciton dissociation lifetime, $\tau_D = 10^{-9}$ s. For this range of dissociation lifetime, the generated excitons split into free carriers already in the volume of the absorber which causes the exciton densities become hundred times less than the density of free carriers and the solar cell behaves like a classical bipolar device. Since the electron contact at the left is the only contact that is active in dissociation of excitons to charge carriers, we have used exponential integral in the generation profile to have the maximum generation near this contact as well as to achieve the SQ maximum efficiency. In fact, we have included the nanoparticle absorption to the cell mathematically with this integral term. By moving toward the hole contact two things can happen. First, exciton dissociation and creation of charge carriers due to the low dissociation lifetime, and second, the radiative recombination of the excitons, which both of these events would result to decrease the exciton density beside the right contact.

In contrast, for high dissociation lifetime, $\tau_D = 10^{-4}$ s, as is shown in Fig. 3 the situation is different. In this case, the excitons can only dissociate when they reach to the electron contact and interface dissociation is more efficient than the bulk dissociation. Although, exciton generation is maximum at the left contact, these generated excitons dissociate already at this interface or travel to the right contact due to

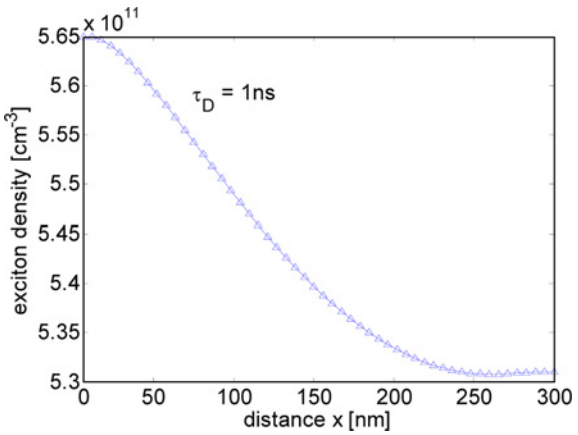

Fig. 2. distribution of excitons inside a p-i-n solar cell for low dissociation lifetime, $\tau_D = 10^{-9}$ s. Excitons decrease exponentially toward the hole contact follow the exponential integral term which is used in generation profile. The parameter used are $\mu_{n,p} = \mu_x = 10^3$ cm^{2}V^{-1}s^{-1}, $S_n = S_{xn} = 10^6$ cms^{-1}.

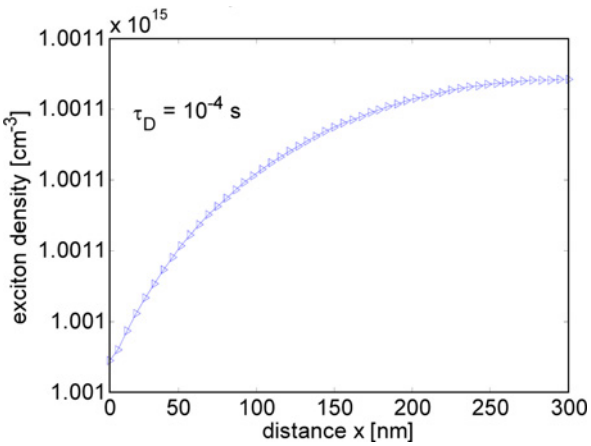

Fig. 3. distribution of excitons in the absorber of a p-i-n-type solar cell for high dissociation lifetime, $\tau_D = 10^{-4}$ s. The parameter used are $\mu_{n,p} = \mu_x = 10^3$ cm^{2}V^{-1}s^{-1}, $S_n = S_{xn} = 10^6$ cm s^{-1}.

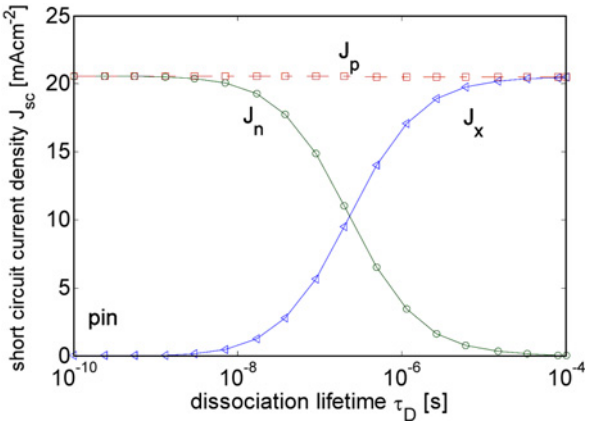

Fig. 4. short circuit current density as a function of exciton dissociation lifetime for a p-i-n type solar cell. Efficient coupling between excitons and charge carriers, low τ_D, leads to bipolar transport, while an inefficient coupling forces the current to be transported by excitons to the contact.

the high dissociation lifetime. In other words, for high dissociation lifetime the generated excitons would have enough time to travel to the hole contact and contribute to excitonic current which result to an increase in density of exciton at the right contact, e.g., energy transport via excitons is more efficient than drift-diffusion transport of charge carriers. This limit corresponds to the situation of an excitonic solar cell as defined by.[17,18]

A more detailed analysis of this transition is depicted in Fig. 4. As can be seen from this figure, for a short dissociation lifetime $\tau_D < 10^{-8}$ s, the device acts like a classical p-i-n-solar cell, where the charge separation basically takes place within the bulk of the absorber and with the help of the built-in field.

This is because in this situation the photogenerated excitons dissociate faster than they diffuse to the surface and also faster than they recombine with their radiative lifetime. In order to achieve this bipolar transport we choose our parameters like equilibrium concentrations, mobilities, dissociation and collection velocities such that exciton dissociation and carrier transport become faster than exciton diffusion and exciton recombinations. In contrast, for $\tau_D > 10^{-5}$ s, the total current of the device is carried by excitons towards the front surface where the short circuit current is generated via interfacial charge separation i.e., excitonic transport is now more than the bipolar transport due to the slow bulk dissociation. In this limit device behave like an "excitonic" solar cell. The transition between the excitonic and the bipolar operation mode occurs at approximately, $\tau_D = 2 \times 10^{-7}$ s. This transition from bipolar to excitonic transport not only depends on exciton dissociation and radative recombination lifetime but also on the respective mobility of the excitons and the charge carriers as well as on the interface dissociation and collection velocities. For this situation we find that J_x and that J_n are

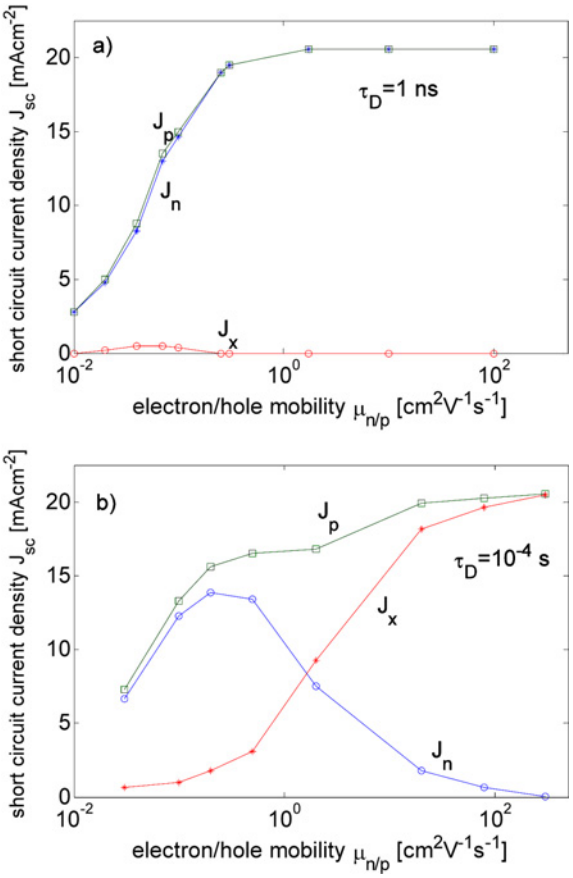

Fig. 5. Short circuit current density for different values of the electron and hole mobilities $\mu_n = \mu_p$ for a p-i-n-type device with a fix exciton mobility $\mu_\chi = 10^{-3}$ cm^2 V^{-1}s^{-1} for all data points. a) τ_D = 1ns, corresponds to the bipolar case in which the electron current J_n decreases and the excitonic current J_x is not capable of compensating this loss. b) τ_D = 100 ms, corresponds to the excitonic case in which the excitonic current starts to decrease already at $\mu_p \approx 2 \times 10^2$ cm^2 V^{-1}s^{-1}. Although μ_n is decreasing parallel to μ_p, J_n partly compensates the loss in J_x, before at mobilities $\mu_{n,p} < 10^{-1}$ cm^{2}V^{-1}s^{-1} all contributions to the short circuit current vanish simultaneously.

unaffected by the choice of $S_{\chi n}$ and S_n as long as $S_{\chi n}$, $S_n > 10^5$ cms^{-1}. We note that, short circuit current density J_{SC} (corresponding to the hole current J_p at $x = d$) is as large as the total number of absorbed photons per unit time. Thus, we have a full photocurrent collection, regardless whether the current is carried by electrons or by excitons. Thus, the SQ theory correctly describes the limiting efficiency for bipolar as well as for excitonic solar cells.

Now, we investigate the effect of small electron and hole mobilities $\mu_{n,p}$ on transport. Obviously, in order to create voltage in solar cells, electrons and holes should travel to their respective contacts and collect there. There are different situations for transport depending on the exciton dissociation lifetime (the places where the excitons dissociate) in organic solar cells. As an example, if excitons dissociate in a place next to the electron contact, there would be a longer distance

for holes rather than electrons to travel to their contact leading to higher hole currents rather than electron currents. This difference between electron and hole current will taken over by excitonic currents. Figure 5 depicts the short circuit current density of a p-i-n-type solar cell as a function of electron/hole mobility with a fix exciton mobility, $\mu_x = 10^3$ $cm^2V^{-1}s^{-1}$, where we are interested to see the combined effect of simultaneously lowering both electron and hole mobility. Since the only allowed contact for dissociation of excitons is the electron contact, the total current at the backside is carried by holes. Consequently, low hole mobilities always lead to a decline of the total current, though the mobility of excitons μ_x is kept as high as $\mu_x = 10^3$ $cm^2V^{-1}s^{-1}$. The intermediate region, between totally quenched short circuit current and a sufficiently high mobility to collect all created electron/hole pairs, shows different effects depending on the dissociation lifetime. Figure 5(a) represent the case of the low dissociation lifetime, $\tau_D = 1$ ns (bipolar case in Fig. 4) where for high mobilities, the short circuit current at $x = 0$ is carried by electrons. Since this τ_D corresponds to a bipolar device, The exciton component J_x plays no role in this situation and lowering the values of $\mu_{n,p}$ leads to an almost synchronous decline of J_n and J_p starting at $\mu_{n,p} \approx 3 \times 10^{-1}$ $cm^2V^{-1}s^{-1}$. In contrast, for $\tau_D = 100$ μs (Fig. 5(b)), the situation is different and the exciton current J_x dominates at $\mu_{n,p} > 2 \times 10^2$ $cm^2V^{-1}s^{-1}$. Lowering $\mu_{n,p}$ below this value decreases the contribution J_x whereas J_n increases. This is due to the fact that high exciton mobility creates a high exciton current J_x at $x = 0$ as well as exciton dissociation at the light exposed surface. This exciton dissociation at the electron contact leads to a hole in the bulk of the absorber directly next to the contact which enforces a hole current through the entire thickness of the device. In contrast, dissociation of the excitons into electrons and holes in the bulk (leading to a high electron current J_n at $x = 0$) allows for a shorter way for the holes to the back contact. However, a further decrease of the mobilities $\mu_{n,p} < 10^{-1}$ $cm^2V^{-1}s^{-1}$ of the electrons and holes leads to a total decline of all contributions to the short circuit current.

In the next step, we discuss the effect of band offset on transport. The open circuit voltage of most real solar cells is controlled by non-radiative recombination at defects and interfaces. As a direct consequence, the band offset δE_C between conduction band of donor and acceptor molecule and the morphology,[29] i.e. the average distance w between two heterointerfaces, become decisive parameters for the efficiency of the solar cells. Interestingly, both parameters bear a trade-off between optimizing dissociation of excitons, favored by low values of w and large band offsets δE_C, and the minimization of recombination losses, requiring large distances w and band offsets as small as possible. In the following we focus on the band offset at the interface and assume that the transport of excitons to the interface and the collection of electrons and holes are efficient.

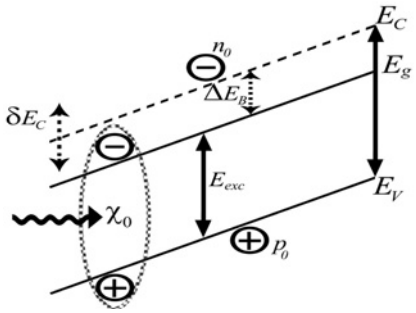

Fig. 6. band diagram of a p-i-n type solar cell showing that a relative shift δE_C of the conduction band is equivalent in a change to exciton binding energy.

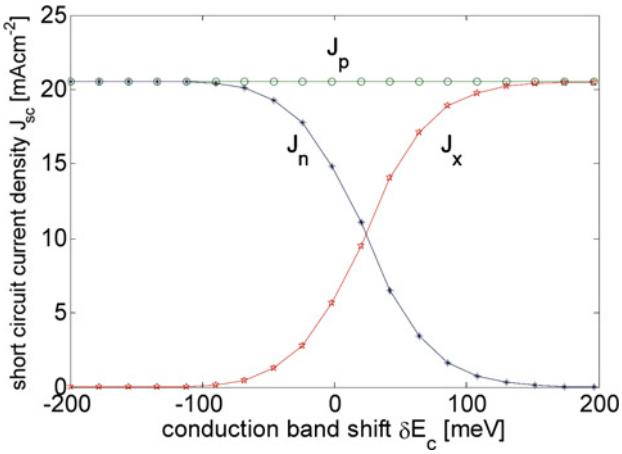

Fig. 7. variation in the short circuit current density resulting from the relative shift δE_C of the conduction band for the free electrons in the volume for the case of a p-i-n type device. Shifting the conduction bands leads to a change in electron equilibrium concentrations n_0 and thus, to a change in dominating transport mechanism.

Besides the coupling constant τ_D between excitons and free carriers, also the equilibrium concentrations of excitons and free carriers affect the dominant charge separation pathway. Note that the ratio between those equilibrium concentrations is determined by the binding energy ΔE_B of the exciton. In order to keep the energy E_{exc} of the excitons and, therefore, the overall absorptance as well as the maximum short circuit current constant, we shift the energy E_C by a relative amount δE_C as illustrated in Fig. 6. A lowering of E_C at constant E_{exc} means that the binding energy ΔE_B of the exciton becomes smaller and vice versa.

Figure 7 shows a simulation, where the conduction band edge and consequently the equilibrium concentration of electrons in the volume of the device varies. Note that the conduction band at the contact is not changed in order to avoid intermixing of additional effects due to enhanced or deteriorated extraction of excitons and carriers at the contact. In thermal equilibrium, the recombination of electrons and

holes equals the dissociation of excitons, leading to

$$H_\chi n_0 p_0 = S_\chi \chi_0 \quad (13)$$

where H_x defines the recombination rate and S_x the dissociation rate. Note that S_x describes the interaction between excitons and free carriers. The equilibrium concentrations n_0 and p_0 of electrons and holes will depend on the band gap of the respective material. If we now vary the conduction band energy E_C, the equilibrium concentration of charge carriers will change. If everything else is kept constant, then an increase in E_c implies a high ΔE_B and, thus, a low equilibrium concentration n_0. The validity of Eq. (13) requires that the dissociation rate S_x also changes with the band offset, since χ_0 stays constant. The latter is a useful assumption since changing χ_0 would also mean that the absorption in the solar cell would change. So, the dissociation is more efficient if the ΔE_B is low. If the conduction band is lifted up, the equilibrium concentration of electrons as well as the interaction between excitons and free charge carriers is diminished and thus, the photocurrent becomes predominantly excitonic. In contrast, when the conduction band energy is lowered, there are more electrons in the absorber available to carry the current and thus, the balance shifts in direction of the bipolar current.

Note that the choice of R_x leads to $\tau_D = 10^{-7}$ s for $\delta E_C = 0$, such that direct comparison is possible with Fig. 4. Shifting the conduction band up lowers n_0 and makes transport via excitons becomes more favorable. In order not to affect the extraction of excitons and carriers at the contacts and the built-in voltage, the equilibrium concentrations in the contacts are not changed and mark the zero position in the δE_C axis.

Finally in the last step, we investigate the validity of the reciprocity theorem between quantum efficieny and electroluminescence as defined by Eq. (9). Figure 8 shows the comparison of directly measured quantum efficiency $Q_{e,dir}$ and the quantum efficiency $Q_{e,EL}$ derived from the electroluminescence measurement (The physical concept of the Eq. (9)) for two different exciton mobility. The electroluminescence (EL) emission simulated with the model described above allows us to derive the quantum efficiency via Eq. (9). As is shown, for the case of high mobilities the quantum efficiency calculated from the EL (solid line) agrees with the directly simulated quantum efficiency (open rectangles). Thus, for perfect transport the reciprocity theorem is valid in both excitonic and bipolar solar cells no matter whether the device is built as p-i-n-type or p-n-type device. Proceeding now to less ideal devices, we investigate under which circumstances the reciprocity relation begins to lose its validity. Fig. 8 also shows that for the case of low mobility the quantum efficiency derived from the EL spectrum via the reciprocity theorem (solid) follows the directly simulated quantum efficiency (open circles) of the solar cell. Since this configuration leads to a relatively constant photocurrent and ideal recombination current, also the reciprocity is valid.

Starting with the limit of high carriers mobilities we discuss in the following how restrictions for excitonic and/or bipolar transport affect the validity of the reciprocity theo-

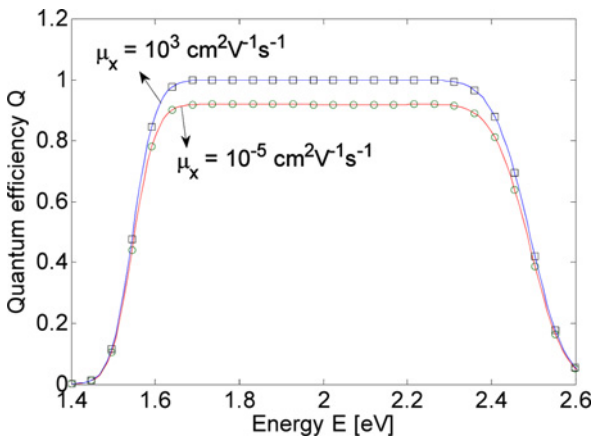

Fig. 8. Quantum efficiency calculated from the El according to Eq. (9) and Quantum efficiency for an ideal solar cell with the parameters, $\mu_{n,p} = 10^3$ cm^{2}V^{-1}s^{-1} and $\tau_D = 10^{-4}$ s. for both devices the reciprocity theorem is valid.

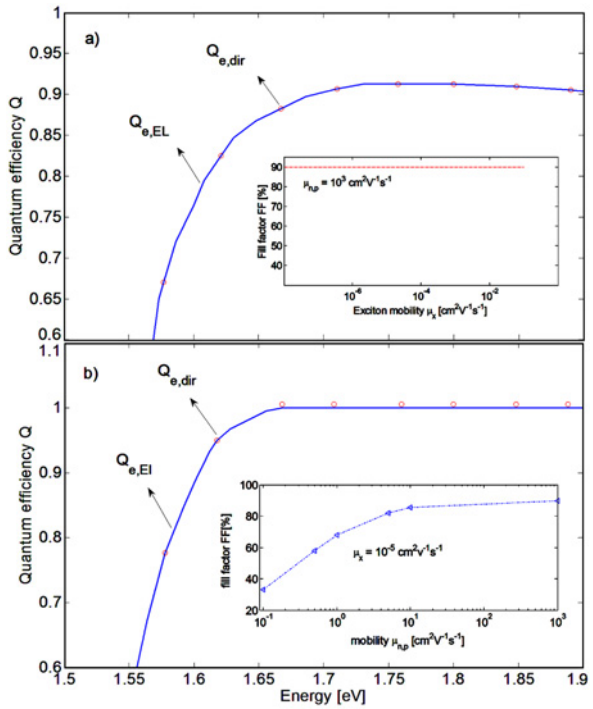

Fig. 9. Summary of the effects of reduced bipolar and excitonic mobilities on simulation of the quantum efficiency $Q_{e,dir}$ (circles) compared with the simulation of the electroluminescence spectrum, from which the quantum efficiency $Q_{e,EL}$ (solid line) is calculated using Eq. (9), for the case of (a) excitonic solar cell and (b) bipolar solar cell. For case (a), the electron and hole mobility are high ($\mu_{n,p} = 10^3$ cm^{2}V^{-1}s^{-1}) and thus collection and injection of carriers is voltage independent and the reciprocity is valid. For case (b), the low bipolar mobility leads to a small deviation between $Q_{e,dir}$ and $Q_{e,EL}$.

rem. Figure 9 summarizes the validity of the reciprocity theorem by comparing the directly simulated quantum efficiency $Q_{e,dir}$ (circles) and the quantum efficiency $Q_{e,EL}$ calculated from the simulation of the EL (solid lines) for the two cases of excitonic and bipolar solar cells. Figure 9(a) depicts simulation results of a case of excitonic solar cell. For this case the electron and hole mobilities are high and thus the reciprocity is valid although the quantum efficiency is below unity in the saturation regime. As is shown in the inset of Fig. 9(a), the fill factor is high and independent from the exciton mobility which implies voltage independent collection and injection of carriers at high bipolar mobilities and the validity of the reciprocity relation ($Q_{e,dir} = Q_{e,EL}$).

Figure 9(b) shows a case of bipolar device with an efficient coupling between excitons and free carriers in which the reciprocity is no longer valid ($Q_{e,dir} \neq Q_{e,EL}$). We learned from inset of Fig. 9(b) that fill factor decreases around $\Delta FF = 3\%$ compared to the high mobility case resulting from decreasing the charge carrier mobility. In consequence, we also find a small deviation of quantum efficiency $Q_{e,dir}$ (circles) and quantum efficiency $Q_{e,EL}$ from EL (solid line), as shown in Fig. 9(b). Note here that the voltage dependence of the carrier collection probability from the 300-nm thick absorber shows up at high forward bias voltage V (leading to FF losses) makes the EL spectrum a function of applied voltage. The voltage used for all EL spectra in Figs. 8 and 9 is $V = 1$ V. Using higher (lower) voltages would increase (decrease) the difference between direct quantum efficiency simulated at $V = 0$ V and quantum efficiency calculated from EL.

4. CONCLUSIONS

The present paper has introduced a model for solar cells that connects the Shockley-Queisser theory to the classical diode theory and includes transport and interaction of excitons, electrons, and holes. In order to drive this model we solve the continuity equations numerically. The model is designed to be compatible with the SQ efficiency limit. Also the model is able to describe a continuous transition between an excitonic and a bipolar operation mode of p-i-n-as well as p-n-type solar cells. The paper describes the effect of charge carriers mobilities on short-circuit current for two cases of excitonic and bipolar cells and shows that it is not possible to have an excitonic device that does not rely also on a sufficient mobility of at least one type of the charged particles. We have discussed the effects of band offsets on transport. In this case, we see a transition from bipolar to excitonic transport with increasing the conduction band offset. This paper also shows that the transport is voltage-dependent for bipolar case while for cells with mainly excitonic transport, no voltage dependencies are apparent since exciton diffusion does not depend on the built-in field. The difference in voltage dependence is reflected in the validity of the fundamental reciprocity of photovoltaic quantum efficiency and electroluminescent emission of solar cells. For voltage-dependent collection and injection, the reciprocity is no longer valid, which is proven by the simulation of electroluminescence and quantum efficiency spectra. This model is able to account for the device specific aspects of a variety of solar cells and provides a means to determine fundamental efficiency limits as well as to simulate practical devices with one common model. The devices that can be described with this model include all types of inorganic solar cells, quantum dot and quantum well solar cells with some simplifications and organic bulk heterojunction solar cells. One important candidate for future work is the dye-sensitized solar cell.

REFERENCES

1. N. S. Levis, *Science* **315**, 798 (2007).
2. M. Green, K. Emery, Y. Hishikawa, W. Warta, and E. Dunlop, *Progress in Photovoltaics: Research and Applications*. **19**, 565 (2011).
3. H. M. Stec, R. J. Williams, T. S. Jones, and R. A. Hatton, *Adv. Funct. Mat*. **21**, 1709 (2011).
4. H. Park, J. A. Rowehl, K. K. Kim, V. Bulovic, and J. Kong, *IOP Science Nanotechnology* **21**, 50 (2010).
5. H. Lu, B. Akgun, and T. B. Russell, *Adv. Eng. Mat*. **1**, 870 (2011).
6. Y. Kim, S. Cook, S. M. Tuladhar, S. A. Choulis, J. Nelson, J. R. Durrant, D. D. C. Bradley, M. Giles, I. McCulloch, C-S. Ha, and M. Ree, *Nature. Mater.* **5**, 197 (2006).
7. J. Y. Kim, K. Lee, N. E. Coates, D. Moses, T-Q. Nguyen, M. Dante, and A. J. Heeger, *Science* **317**, 222 (2007).
8. J. Peet, J. Y. Kim, N. E. Coates, W. L. Ma, D. Moses, A. J. Heeger, and G. C. Bazan, *Nat. Mater*. **6**, 497 (2007).
9. S. Bertho, G. Janssen, T. J. Cleij, B. Conings, W. Moons, A. Gadisa, J. D'haen, E. Goovaerts, L. Lutsen, J. Manca, and D. Vanderzande, *Sol. Energy. Mater. Sol. Cells*. **92**, 753 (2008).
10. A. Yella, H.-W. Lee, H. N. Tsao, C. Yi, A. K. Chandiran, M. K. Nazeeruddin, E. W.-G. Diau, C.-Y. Yeh, S. M. Zakeeruddin, and M. Gratzel, *Science* **334**, 629 (2011).
11. S. Zhang, C. Ji, Z. Bian, R. Liut, X. Xia, D. Yun, L. Zhang, C. Huang, and A. Cao, *Nano. Lett*. **11**, 3383 (2011).
12. M. Law, L. E. Greene, J. C. Johnson, R. Saykally, and P. Yang, *Nat. Matter*. **4**, 455 (2005).
13. L. Schmidt-Mende, U. Bach, R. Humphry-Baker, T. Horiuchi, H. Miura, S. Ito, S. Uchida, and M. Gratzel, *Adv. Mater*. **17**, 813 (2005).
14. J. Schrier, D. O. Demchenko, L.-W. Wang, and A. P. Alivisatos, *Nano. Lett*. **7**, 2377 (2007).
15. C.W. Tang, *Appl. Phys. Lett*. **48**, 183 (1986).
16. M. A. Green, *Physica. E*. **14**, 65 (2002).
17. B. A. Gregg and M. C. Hanna, *J. Appl. Phys*. **93**, 3605 (2003).

18. B. A. Gregg, *J. Phys. Chem. B.* **107**, 4688 (2003).
19. R. Corkish, D. S. P. Chan, and M. A. Green, *J. Appl. Phys*. **79**, 195 (1996).
20. M. Burgelman and B. Minnaert, *Thin. Solid. Films* **511**, 214 (2006).
21. W. Shockley and H. J. Queisser, *J. Appl. Phys*. **32**, 510 (1961).
22. M. A. Green, *Solar Cells: Operating Principles, Technology, and System Applications*, p. 62, Prentice-Hall, Englewood Cliffs, New Jersey (1982).
23. W. Shockley, *Bell. Syst. Tech. J*. **28**, 435 (1949).
24. A. Marti, J. L. Balenzategui, and R. F. Reyna *J. Appl. Phys*. **82**, 4067 (1997).
25. J. Mattheis, J. H. Werner, and U. Rau, *Phys. Rev. B*. **77**, 085203 (2008).
26. C. Donolato, *Appl. Phys. Lett*. **46**, 270 (1985).
27. T. Markvart, *IEEE. Trans. Electron. Devices* **43**, 1034 (1996).
28. J. Rostalski and D. Meissner, *Sol. Energy Mater. Sol. Cells*. **63**, 37 (2000).
29. H. Hoppe and N. S. Sariciftci, *J. Mater. Chem*. **16**, 45 (2006).